Photonic quasicrystals exhibit zero-transmission regions due to translational arrangement of constituent parts

Han Zhao,[1] Remo Proietti Zaccaria,[1,2,*] Jun-feng Song,[1] Satoshi Kawata,[2] and Hong-bo Sun[1]
[1]*State Key Laboratory on Integrated Optoelectronics, College of Electronic Science and Engineering, Jilin University, 2699 Qianjin Street, Changchun 130012, People's Republic of China*
[2]*Department of Applied Physics, LaSIE, Osaka University, 2-1 Yamada-Oka, Suita, Osaka 565-0871, Japan*
(Received 23 April 2008; revised manuscript received 30 August 2008; published 19 March 2009)

We have investigated the origin of the optical zero-transmission regions in different kinds of highly symmetric quasicrystal structures. We report on the possibility of reproducing the same optical characteristics by using some of the constituent parts of the quasicrystals, arranged in standard photonic crystal geometries showing translational symmetry. This finding represents a challenge to the common assumption that high-order symmetry is the reason for the large optical zero-transmission regions shown by quasicrystals. This insight into the field of quasiperiodic photonic devices opens up key questions about opportunities for quasicrystals in optical applications.

DOI: 10.1103/PhysRevB.79.115118 PACS number(s): 42.70.Qs, 78.20.Bh

I. INTRODUCTION

Photonic crystals are structures with a periodic modulation of the refractive index profile. The existence of a gap in the transmission spectrum (TS) of such structures provides an opportunity to confine and control the propagation of electromagnetic waves.[1,2] It has been recognized that a photonic band gap can exist, in terms of zero-transmission region, not only in periodic lattices, but also in quasicrystals.[3–6] This kind of structure has neither true periodicity nor translational symmetry, but shows a quasiperiodicity which exhibits high-order rotational and mirror symmetry.[7] Photonic quasicrystals (PQCs) have received an increasing amount of attention in recent years. The transmission properties of many kinds of PQCs with 8-fold,[8,9] 10-fold,[10,11] and 12-fold[4,12–14] symmetries in two dimensions have been calculated. Moreover, experimental investigation of three-dimensional structures was also recently reported.[15,16] These studies have demonstrated that most PQCs possess wide zero-transmission regions. It is claimed that particularly large optical gaps are found in 12-fold symmetric quasicrystals because of the high symmetry shown by those structures. In this paper, we challenge such statements, concentrating our efforts on studying different forms of 12-fold photonic quasicrystals. We will show that photonic crystals, obtained by arranging some of the quasicrystals' constituent parts in a translational symmetry pattern (*constituent parts method*), can reproduce the *same* optical (characteristics) structures realized by PQC, which leads us to conclude that periodic and quasiperiodic structures manifest a similarity much stronger than what is usually recognized. This, in turn, must therefore reduce the role played by the high degree of symmetry shown by PQC. It is interesting to notice that this approach agrees on some level with the approximant studies of electronic systems.[17] According to this method it is possible to identify an infinite countable set of structures which tend to reproduce the same electro-optical properties of the quasicrystal itself.[18] Their main characteristic is to show translational symmetry in a higher-dimensional space than the quasicrystal. Because of this peculiarity, they are relatively easy to investigate by means of a band-structure analysis and this may be helpful in gaining some insights into the properties of the associated quasicrystal. Hence, both the constituent parts method and the approximant approach involve the analysis of periodic lattices in some manner related to the quasicrystal. However, while the approximant approach takes into consideration structures which are similar but not equal to the quasicrystal, the constituent parts method studies particular pieces of the quasicrystal which, by definition, do actually exist inside the quasiperiodic structure. In other words, the approximant method looks for a general periodic structure which can describe the properties of a quasicrystal, whereas our method focuses on the optical properties of parts of the quasicrystal which assembled together reproduce the quasiperiodic structure exactly. Considering these two diametrically opposite approaches, the constituent parts method is inevitably connected to the short-range properties of the quasicrystal. As we shall see, this is an important condition (but not sufficient) for the constituent parts to assure the creation of a zero-transmission region in the quasicrystal. On the other hand, this aspect cannot be described by the approximant method, which tends to miss some of the local information of a quasicrystal.

II. STRUCTURE

Two kinds of patterns will be investigated: Stampfli and Penrose dodecagons. These are shown in Fig. 1. The first [Fig. 1(a)] was built up following the random-Stampfli inflation rules,[4,19] which show self-similarity properties. This means that starting from a structure characterized by some symmetries, they will be maintained by an enlarged similar structure. Figure 2 shows the process of forming a Stampfli quasicrystal. Two basic cells, a square and a triangle, are arranged to realize the 12-fold symmetry. Starting from the center of the figure and moving to the outer regions, its 19 points have the coordinates (0,0), $[(\pm\sqrt{3}/2,\pm 1/2),(0,\pm 1)]$, and $[(\pm(1+\sqrt{3}/2),\pm 1/2),(\pm 1/2,\pm(1+\sqrt{3}/2)),(\pm(1/2+\sqrt{3}/2),\pm(1/2+\sqrt{3}/2))]$. Next, by zooming out of $2+\sqrt{3}$ (the equivalent of the golden ratio for Penrose tilings) and

 ©2009 The American Physical Society

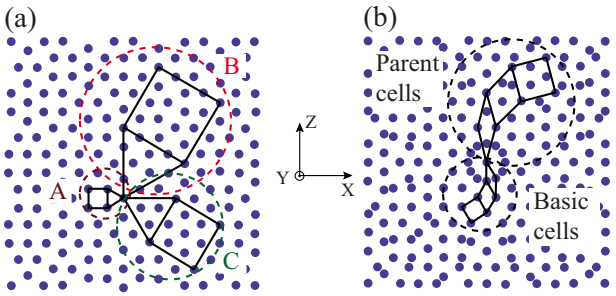

FIG. 1. (Color online) (a) Stampfli 12-fold quasicrystal. From left, proceeding clockwise, are shown the two basic cells [small square and triangle (A)] and two different families of parent cells (B and C). (b) Penrose 12-fold quasicrystal. Three basic cells, a square and two kinds of rhombi, are shown at the bottom of the figure. At the top, a set of parent cells is highlighted.

substituting each point of Fig. 2(b) with the cell of Fig. 2(a), a larger quasicrystal is obtained, as shown in Fig. 3. In the end, by repeating the previous steps the structure can be enlarged indefinitely.

From a modeling point of view we have chosen to represent the Stampfli structure as a quasiperiodic sequence of holes in a solid background made of Si. The dimensionality along the direction parallel to the axis of the holes is considered infinite, which makes the system a virtually two-dimensional structure. Although such approximation is unrealistic from a practical point of view, it does not affect the in-plane optical gaps which are mainly related to the two-dimensional properties of these lattices and, at the same time, it results in speeding up our simulations. The lattice constant is $a=350$ nm and holes are of radius $r=0.3a$. The refractive index of the background is 3.477. Moreover, the imaginary part of the refractive index is taken equal to zero. Such assumption is justified because of our particular interest in the telecommunication wavelength range ($\lambda \approx 1.55$ μm), where light absorption from silicon can be neglected.

The second simulated pattern we use is also a two-dimensional representation of a special configuration of the Penrose dodecagon. Different from the Stampfli structure, here three basic cells are necessary to build the quasicrystal: a square and two rhombi having acute angles of 30° and 60°, respectively.[20] From the figure the geometrical differences between the two structures are immediately apparent, even though both manifest 12-fold symmetry. It is also worthwhile to mention the existence of different geometrical configurations that can represent dodecagons besides the two patterns illustrated here. The main difference with these are in the shape of the basic constituent parts which realize the quasicrystal.[20–24] As we will describe later in detail, for the calculations of the Penrose structure we have chosen a configuration complementary to the Stampfli one, in the sense that cylinders in air have been taken.

The range of the simulation models is 8.0 μm $\times \infty$ $\times$ 8.0 μm (x,y,z) for both the Stampfli and Penrose structures. Specifically, the rigorous coupled wave analysis (RCWA) is used in all the simulations. This kind of approach, even though it is known for its efficiency in solving two-dimensional structures with translational periodicity, has given also extremely satisfactory results for quasicrystals. Moreover, for its own nature, it is capable of an automatic normalization of the transmitted signal which results in a simplification of the simulations compared to a more canonical finite difference time domain (FDTD) approach. We have actually solved the systems discussed here with both the methods and they agree in the results (however we have chosen to show only the RCWA simulations).[25]

The domain is large enough to guarantee convergent results, meaning that even when enlarging the structures there is no shifting of the zero-transmission regions. We use a sequence of plane waves to address the problem of transmission width in the integrated quasicrystal. As mentioned, the interval of frequencies is chosen to fall in the telecommunication range.

A. Contributions to the zero-transmission regions: The Stampfli quasicrystal

In Fig. 4 we show the transmission spectrum of the 12-fold Stampfli quasicrystal of air holes in Si. In particular, because no zero-transmission regions are obtained for the TM case, only the TE polarization is plotted (electric field parallel to the x-z plane). Figure 4 shows the TS along directions with angles of 0°, 5°, 10°, 15°, 20°, 25°, and 30° from

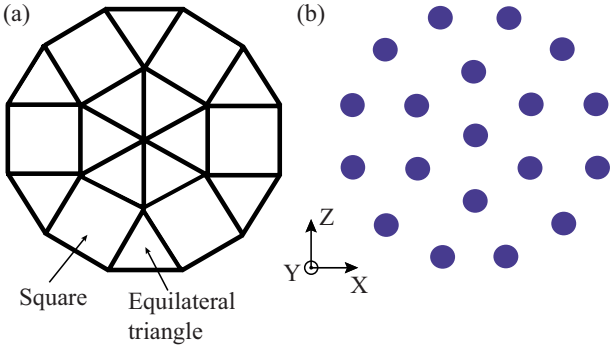

FIG. 2. (Color online) (a) The two basic constituent parts, square and equilateral triangle, of a 12-fold Stampfli quasicrystal forming the core of the structure. (b) Only the vertices of squares and triangles are highlighted.

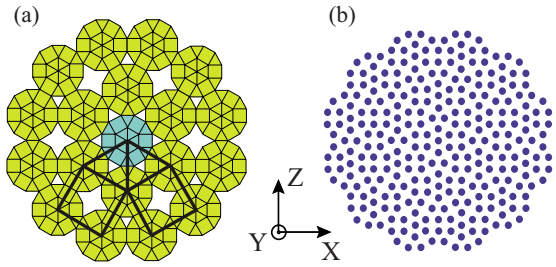

FIG. 3. (Color online) (a) 19 dodecagonal cores have been put together to enlarge the 12-fold Stampfli quasicrystal. It is interesting to notice that the parent cells (thick lines), which correspond to family B in Fig. 1(a), have the same symmetry as the basic cells. The ratio between the sides of the parent and basic cells is $2+\sqrt{3}$. (b) The 12-fold quasicrystal when two steps of the Stampfli inflation are taken.

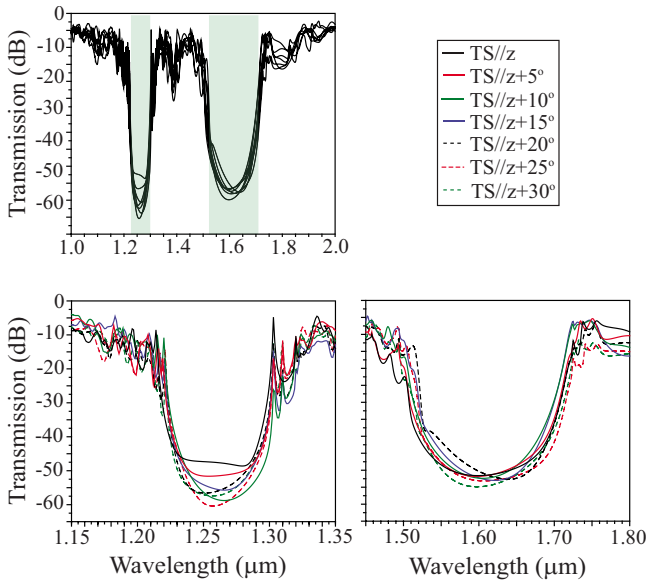

FIG. 4. (Color online) TS of 12-fold Stampfli PQC consisting of air holes in silicon along 0°, 5°, 10°, 15°, 20°, 25°, and 30° angles from the z direction for the TE mode. Two zero-transmission regions centered at 1.26 and 1.62 μm are identified (opaque background). Specifically, the ranges are [1.22,1.30] and [1.52,1.71] μm. Enlargements of the zero-transmission regions are shown.

the z axis. Furthermore, because of the 12-fold characteristic of the quasicrystal, many more angles are included in the previous ones. For example, a 20° angle corresponds to 80° from the z axis. From the figure we can see that the zero-transmission regions of the Stampfli quasicrystal can be identified by looking along the directions of high symmetry of the structure (0°, 15°, and 30°).[4] A heuristic explanation can be given when we consider that the Fourier transform of a crystal, namely, its pattern in the reciprocal space, is still invariant for discrete translations. Because the structure in the real space repeats itself with a modulation given by the lattice constant, we can define a part of it (unit cell) which will be enough to describe the physical properties of the complete periodic structure. In terms of Fourier transform, it means we have to deal with only the first Brillouin zone. If now we shift our attention to the origin of the high-symmetry lines in the Brillouin zone, we see that they depend on the rotational and inversion symmetries of the crystal in the real space. In a quasicrystal there is no translational periodicity but still its Fourier transform is well defined; namely, we can move from real space to the reciprocal and vice versa. Of course, for a quasicrystal we can also define its own rotational and inversion symmetries which will be transported in its reciprocal space through a Fourier transformation. However, different from standard crystals, now there is no translational periodicity so we cannot identify a smaller section of the quasicrystal to reproduce its physical characteristics. Hence, to identify the reciprocal of a quasicrystal the Fourier transform of the complete structure is necessary. In other words, for a quasicrystal the concepts of unit cell and total structure can be considered equivalent. In this perspective, we can then identify high-symmetry lines in the reciprocal

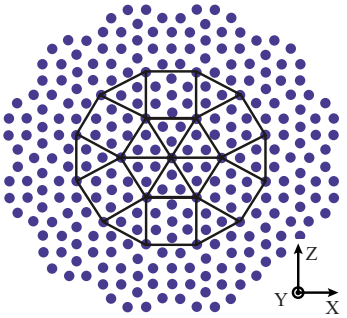

FIG. 5. (Color online) 12-fold Stampfli quasicrystal with parent family C highlighted. This family has the characteristic of being able to fill completely the space of the quasicrystal. The ratio between the sides of parent and basic cells is $1+\sqrt{3}$.

space similarly to what is done for perfect crystals with the difference that they will be not confined in space (in comparison, a canonical Brillouin zone has well-defined spatial dimensions related to the unit cell in the real space). Finally, if we combine these last considerations with the fact that zero-transmission regions can be localized in crystals simply by looking along high-symmetry directions, we can conclude that also in quasicrystals it is indeed enough to observe transmission along the high-symmetry lines to obtain a full description of the zero-transmission regions.

In the telecommunication frequency range, two optical TE gaps are identified. The first extends from 1.22 to 1.30 μm, whereas the second is seen from 1.52 to 1.71 μm. Because these zero-transmission regions are manifested independently by the direction of the incident light, they represent *full* zero-transmission regions. We interpret this result as a first indication that a 12-fold PQC could have realistic applications for telecommunication purposes.

In Fig. 1(a) three sets of constituent parts making the Stampfli photonic quasicrystals are shown. In particular, a *basic* set and two *parent* sets are highlighted. We have introduced family C by simply revaluating the ratio between the sides of the parent cells and the sides of the basic cell in $1+\sqrt{3}$ versus $2+\sqrt{3}$ for the standard family B. Another difference between the two families is that while C can completely fill the whole space (see Fig. 5), B needs other kinds of parent cells to reach the same goal. Indeed, the inner geometry of both squares and triangles in family C does not change moving away from the center of the structure, which is not true for family B. Such a difference could suggest the idea that to define the optical properties of the Stampfli quasicrystal, family B, as defined, may be not enough. However, we will show that it is not the case and the present definitions are well put.

In the present work we select each of these families to construct six *translational* periodic structures by arranging the cells into triangularlike and squarelike lattices as depicted in the insets of Fig. 6. More precisely, we fill the entire space following triangular, square, rhomboidal, and rectangular configurations. To perform the correct calculations, it is important to identify the proper Brillouin zones and hence the directions of high symmetry corresponding to the simulated crystals. A closer look at Fig. 6(c) reveals that

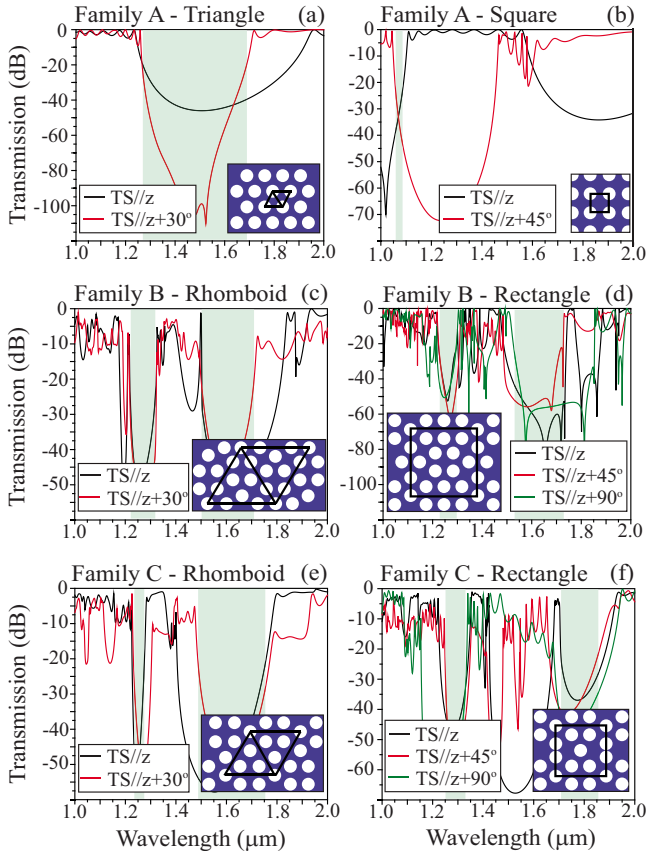

FIG. 6. (Color online) Transmission spectra of the three simulated families for the Stampfli quasicrystal. The ranges of the zero-transmission regions, highlighted in the figure, are (a) [1.27,1.69], (b) [1.05,1.09], (c) [1.22,1.32] and [1.50,1.71], (d) [1.22,1.30] and [1.52,1.73], (e) [1.23,1.27] and [1.48,1.76], and (f) [1.25,1.33] and [1.71,1.86] μm. The light is TE polarized. The insets show the corresponding geometries of the simulated photonic crystals.

by choosing a triangular supercell as the primitive cell, this would not allow the fulfillment of requirements for a Bravais lattice. Instead, by considering a rhomboidal structure, such requirements can be satisfied. Similarly, Fig. 6(d) can be described by assuming a rectangular primitive cell. Indeed, even though the sides of the cell are equal to one another, suggesting a square, the cell is not invariant under rotation of $\pi/2$, so a rectangular description is needed. This point is particularly important because the directions of high symmetry, which in turn dictate the optical properties of the device, depend on the geometry of the unit cell.

We have hence evaluated the transmission spectrum of six structures [families A, B, and C in Fig. 1(a)]. The calculated spectra are displayed in Fig. 6. From them we can see that the band gap of triangular lattice photonic crystal overlaps nearly most of the first- and higher-order zero-transmission regions in the 12-fold Stampfli structure (Fig. 4). Because the triangular lattice is not the only kind of cell included in the quasicrystal, we can expect some extra contributions arising from the other constituent parts. Furthermore, by comparing Figs. 4 and 6(a) we can assume that these are only higher-order corrections, meaning that the main contribution is due to the triangular constituent part. However, at closer inspection, the transmission spectra of the supercells' constituent parts reveal that our previous hypothesis is not entirely correct. In fact, both Figs. 6(c) and 6(d) show two complete band gaps which manifest a consistent overlap with the zero-transmission regions of the 12-fold quasicrystal. To improve our understanding we focus then on the zero-transmission region at low wavelengths, in the range from 1.22 to 1.30 μm. In Fig. 6 only five structures contribute to the optical gap of the Stampfli quasicrystal: the triangular, the two rhomboid, and the two rectangular crystals, even though the triangle and the rectangle of family C give only a partial overlap. It implies that at least for the lowest gap the supercrystals are primarily responsible in defining the transmission properties of the 12-fold structure.

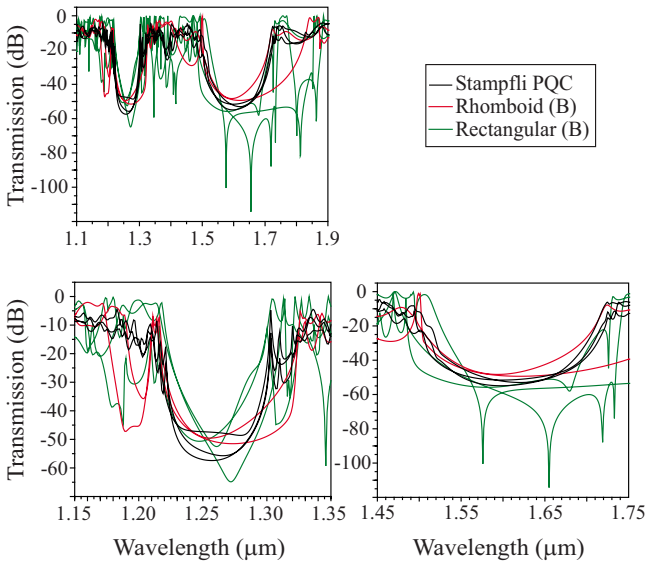

FIG. 7. (Color online) Overlap of the *total* transmission spectra of rectangular and rhomboid photonic supercells of family B. They are compared with the *total* transmission of the Stampfli 12-fold quasicrystal. Lines with same color are associated to the same structure at different angles for the incident radiation (the angles are chosen to have the radiation propagating along the high-symmetry directions). Enlargements of the zero-transmission regions are shown.

The current analysis seems then to lead to the conclusion that supercells are the most important constituent parts of the 12-fold Stampfli quasicrystal. Figure 7 is a visual demonstration of this statement.

The next step to support our results was to calculate the transmission spectra for configurations where all the holes were removed except the ones associated to a particular family (the overall dimensions of the structure are exactly the same as for the quasicrystal). We have done it for both the structures of family B. The transmission spectra are shown in Fig. 8. They confirm what is shown in Figs. 6 and 7: *the transmission spectrum of the Stampfli PQC is well determined by the optical behavior of some of its constituents*.

These results confirm the existence of a strong relation between the optical properties of the 12-fold Stampfli quasicrystal and some of its constituent parts. In particular, all of our simulations point out that certain particular *supercells* arranged with translational periodicity may realize the *same*

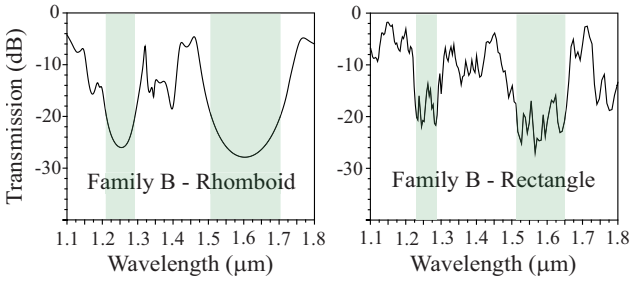

FIG. 8. (Color online) The transmission spectra of the Stampfli quasicrystal when *only* the elements of family B are left. In particular, (a) is for rhomboid and (b) is for rectangular. To each highlighted area corresponds a zero-transmission region. The direction of the incident light was along the x axis. It is interesting to notice the roughness of the profile in (b) compared to (a). It is because of the high amount of defects existing in the rectangular geometry.

zero-transmission regions of the Stampfli dodecagon.

B. Contributions to the zero-transmission regions: The Penrose quasicrystal

In a tentative approach toward generalizing our results, we have considered a different kind of quasicrystal on which to perform similar analysis. The chosen structure is the 12-fold Penrose lattice, visualized in Fig. 1(b). Additionally, the material distribution has also been modified, with this structure presenting rods in air, namely, the inverse of the previous simulation distribution. Because of this choice, only the TM polarization is able to show zero-transmission zones. The geometrical parameters utilized are a lattice constant of $a=400$ nm and rods of radius $r=0.25a$.

From Fig. 9 we do not notice any similarity between the 12-fold Penrose lattice and its *basic* constituents. By means of an inflation procedure we have then identified a set of *parent* cells, which cover the dodecagon area. The transmission spectra of the three parent cells have been calculated and compared with the optical properties of the Penrose dodecagon. The results demonstrate once again that the zero-transmission regions of a quasicrystal can be realized by creating a photonic crystal with one of its constituents. Indeed, the transmission spectrum of Fig. 9(f) shows a surprisingly good match with the spectrum of the dodecagon Penrose lattice [Fig. 9(a)].

III. ANALYSIS AND DISCUSSION

To describe such phenomenon we have followed two approaches: the first assumes the *number* of constituent parts as a fundamental parameter responsible for the quasicrystal optical gap properties; and the second elects their *surface area* as the main factor. However, both trivial considerations about the relation between geometry and optical properties of the structure and our analysis demonstrate that only the second agrees with the presented simulations.

Let us consider first the Stampfli lattice and let us analyze the three families of constituent parts shown in Fig. 1(a). The amounts of coverage areas in the quasicrystal corresponding to the supercells shown in Figs. 6(c) and 6(d) (family B) are

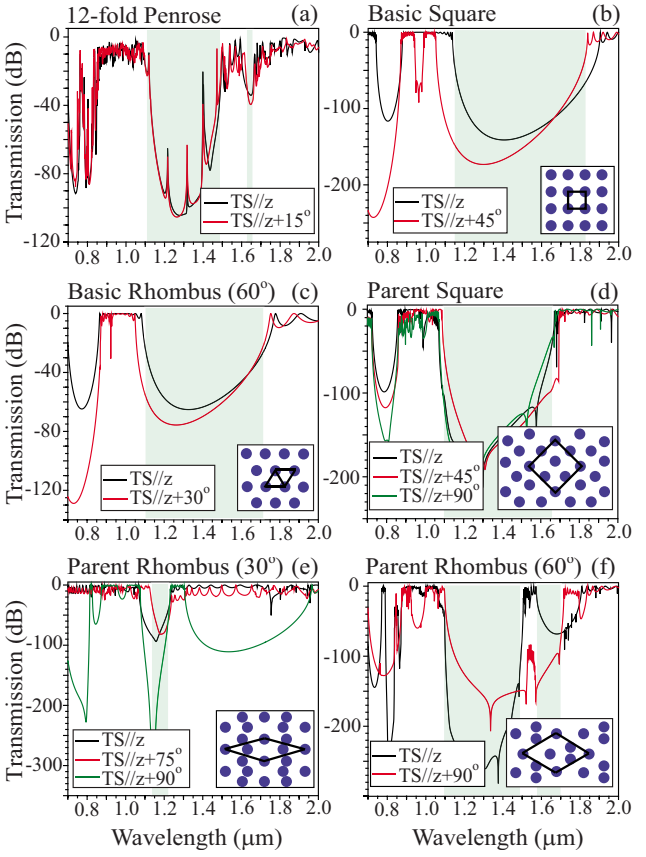

FIG. 9. (Color online) (a) Transmission spectrum of a 12-fold Penrose quasicrystal. A zero-transmission region is found for the TM modes. Accordingly, the present configuration adopts cylinders in air, which facilitates the creation of an optical gap for such modes. The optical gap ranges of interest (highlighted by an opaque area) are [1.10–1.49] and [1.62–1.66] μm. It is interesting to notice the presence of sharp peaks inside the first zero-transmission region. It is signature of defects inside the structure, which is typical in quasicrystals. (b) and (c) show the optical properties of photonic crystals with patterns following the geometry of two out of the three basic constituents of the 12-fold Penrose quasicrystal (the rhombus with 30° acute angle does not realize any optical gap). Specifically (b) is for square and (c) is for rhombus with 60° acute angle. The band gaps are found in the ranges of [1.14–1.83] and [1.10–1.72] μm, respectively. (d)–(f) correspond to the parent set. In detail: (d) parent square, (e) parent rhombus with 30° acute angle, and (f) parent rhombus with 60° acute angle. The insets show the unit cells of the calculated pattern. The different directions of propagation, corresponding to lines of high symmetry, are shown in different colors. The zero-transmission regions for the last three structures are (d) [1.09–1.67], (e) [1.13–1.23], (f) [1.10–1.50], and [1.58–1.71] μm.

54% and 46%, respectively. Because the two values are almost identical, we might expect a similar contribution to the optical behavior of the photonic crystals. In fact, as confirmed by Fig. 7, both the supercells, arranged in a crystal configuration, realize a photonic gap structure extremely close to the Stampfli dodecagon. If we now consider the coverage area of the triangular and square basic cells (family A), the percentages of areas covered are 52% for the square and 48% for the triangle. Accordingly, a similar contribution

to the optical gap of the Stampfli lattice might be expected. However, by looking at Figs. 6(a) and 6(b), we can see that such predictions fail to be confirmed because only the triangular structure seems capable of contributing to the gap. We need to make use of the short-range properties of the cell to explain such an apparent contradiction.[13] Indeed, we easily notice that only the triangular cell shows the same short-range hexagonal symmetry of the Stampfli lattice. Still the question about the reasons which allow family B to reproduce the quasicrystal transmission profile remains unanswered. In order to explain it we must observe the *basic* components forming the geometries in families A and B. Indeed we can see that only the structures in family B are built by using *all* the basic cells (square and triangle; see Fig. 1(a), family A) of the quasicrystal. This is not the case for family A, which explains why they cannot reproduce the same zero-transmission regions of the quasicrystal. Hence, it seems that besides the coverage area and hexagonal short-range symmetry, we must ensure that *all* the basic cells of the quasicrystal exist in the superlattice (crystal made by supercells) for it to able to reproduce a similar transmission spectrum as the quasicrystal. Moving to family C the coverage areas of the two corresponding structures [Figs. 6(e) and 6(f)] are 50% each. Also, both of these possess short-range hexagonal symmetry. However, even though both the structures have same coverage area and short-range symmetry, some substantial differences arise from the simulations of their transmission spectra (family-C-rectangle transmission spectrum does not show a good match with the quasicrystal). To explain the difference in behavior between the two geometries in family C, we must look once again at their basic cells. Indeed, it is interesting to notice that even though both of them possess the two basic cells of the Stampfli quasicrystal, the rectangle supercell shows also an extra basic cell (having the shape of a rhombus with acute angle of 30°). Insight can be gained by comparing the results of family-B and the family-C rhomboids. These three structures show all hexagonal short-range symmetry and they all are formed by the two basic cells of the quasicrystal. Nevertheless Fig. 6(e) shows the worst transmission profile (in terms of overlapping with the quasicrystal) among the three. To explain this result the last consideration must be taken into account: the unit area. Indeed, it is easy to verify that both the structures in family B have a larger area than the rhomboid in family C. In a different way, the area is once again playing an important role in defining the best supercells capable of reproducing the quasicrystal zero-transmission regions.

Analogous analysis has also been carried for the Penrose 12-fold structure. In particular, if we focus our attention on the parent cells, our results indicate percentages of 23.5, 15.6, and 60.9 for rectangle, rhombus-30°, and rhombus-60°, respectively. Clearly, the last shows the strongest presence inside the Penrose lattice, about three or four times more than the other two constituent parts, and also it is the only one containing all the three basic cells of the quasicrystal [see Fig. 1(b)]. This then suggests that the zero-transmission regions of the Penrose 12-fold lattice are defined mainly by the parent rhombus-60°, as confirmed by Fig. 9(f). Furthermore, a comparison between the coverage areas of the parent square (23.5%) and parent rhombus-30° (15.6%) tells us that the former should be able to produce a band structure closer to the quasicrystal than the latter. It is also confirmed by Fig. 9. Finally, none of the three structures shows hexagonal short-range rotational symmetry, which agrees with the discrepancy between the transmission spectra of rhombus-60° and the quasicrystal. Shifting now our attention on the three basic cells, we find that their percentage distributions show similar values. It implies that none of these geometries is able to deeply characterize the quasicrystal. However only the configuration showing short-range hexagonal symmetry (basic-rhombus-60°) is able to realize a band gap which overlaps both the zero-transmission regions of the Penrose quasicrystal.

This analysis, even though it is sufficient to explain the optical behavior of the quasicrystals examined in relation to their own constituent parts, must however be seen as just a heuristic approach. A more detailed analysis could, for example, be performed by considering the relation between the constituent parts of the quasicrystals and their approximant structures. However, such a kind of analysis is not the main goal of the present paper, and it is left for further studies.

In conclusion, we have investigated the origin of the zero-transmission regions of photonic quasicrystals showing high rotational symmetry. The commonly accepted idea that this characteristic is the main reason for large optical zero-transmission regions is reconsidered. We have challenged this concept, by demonstrating that the optical properties of some quasicrystals have their origin in the properties of their constituent parts. According to our considerations, these need only to respect the conditions of being supercells, to be built by using the same basic cells of the quasicrystal and, possibly, they must possess the same short-range rotational symmetry of the quasicrystal.

ACKNOWLEDGMENTS

The authors gratefully acknowledge support from CREST of Japan Science and Technology Agency, and from NSF of China (NSFC) Grants No. 60525412 and No. 60677018.

*Corresponding author; remo@ap.eng.osaka-u.ac.jp

[1] J. D. Joannopoulos, R. D. Meade, and J. N. Winn, *Photonic Crystals: Molding the Flow of Light* (Princeton University Press, Princeton, NJ, 1995).

[2] S. G. Johnson and J. D. Joannopoulos, *Photonic Crystals: The Road from Theory to Practice* (Kluwer, Dordrecht, 2002).

[3] Y. S. Chan, C. T. Chan, and Z. Y. Liu, Phys. Rev. Lett. **80**, 956 (1998).

[4] M. E. Zoorob, M. D. B. Charlton, G. J. Parker, J. J. Baumerg, and M. C. Netti, Nature (London) **404**, 740 (2000).

[5] S. S. M. Cheng, L. M. Li, C. T. Chan, and Z. Q. Zhang, Phys. Rev. B **59**, 4091 (1999).

[6] Strictly speaking the concept of band is a peculiarity of structures with a translational symmetry. However, it is erroneously and commonly used also for quasicrystals where the translational modulation of the refractive index is absent. In this paper we will refer to *band gap* only for structures showing translational symmetry.

[7] D. Levine and P. J. Steinhardt, Phys. Rev. Lett. **53**, 2477 (1984).

[8] J. Romero-Vivas, D. N. Chigrin, A. V. Lavrinenko, and C. M. Sotomayor Torres, Opt. Express **13**, 826 (2005).

[9] J. Romero-Vivas, D. N. Chigrin, A. V. Lavrinenko, and C. M. Sotomayor Torres, Phys. Status Solidi A **202**, 997 (2005).

[10] M. Hase, H. Miyazaki, M. Egashira, N. Shinya, K. M. Kojima, and S. I. Uchida, Phys. Rev. B **66**, 214205 (2002).

[11] M. Notomi, H. Suzuki, T. Tamamura, and K. Edagawa, Phys. Rev. Lett. **92**, 123906 (2004).

[12] X. Zhang, Z. Q. Zhang, and C. T. Chan, Phys. Rev. B **63**, 081105(R) (2001).

[13] Y. Q. Wang, Y. Y. Wang, S. Feng, and Z. Y. Li, Europhys. Lett. **74**, 49 (2006).

[14] K. Nozaki and T. Baba, Appl. Phys. Lett. **84**, 4875 (2004).

[15] W. Man, M. Megens, P. J. Steinhardt, and P. M. Chaikin, Nature (London) **436**, 993 (2005).

[16] A. Ledermann, L. Cademartiri, M. Hermatschweiler, C. Toninelli, G. A. Ozin, D. S. Wiersma, M. Wegener, and G. von Freymann, Nature Mater. **5**, 942 (2006).

[17] C. Janot, *Quasicrystals* (Clarendon, Oxford, 1998).

[18] K. Wang, S. David, A. Chelnokov, and J. M. Lourtioz, J. Mod. Opt. **50**, 2095 (2003).

[19] M. Oxborrow and C. L. Henley, Phys. Rev. B **48**, 6966 (1993).

[20] Y. Wang, X. Hu, X. Xu, B. Cheng, and D. Zhang, Phys. Rev. B **68**, 165106 (2003).

[21] F. Gahler, in *Quasicrystalline Materials*, edited by C. Janot and J. M. Dubois (World Scientific, Singapore, 1988), pp. 272–284.

[22] F. Gahler, R. Luck, S. I. Ben-Abraham, and P. Gummelt, Ferroelectrics **250**, 335 (2001).

[23] J. E. S. Socolar, Phys. Rev. B **39**, 10519 (1989).

[24] A. Yamamoto, Acta Crystallogr., Sect. A: Found. Crystallogr. **52**, 509 (1996).

[25] In our simulations the RCWA method results to be more suitable than the FDTD approach. The reason is doublefold: necessity of lower memory and exact normalization of the signal. For FDTD, the simulation required about four times more memory than the RCWA counterpart. Indeed, because the simulation is two dimensional, we had to make use of four detectors measuring the Poynting vector in order to normalize the transmission. Moreover, it was the complication in the FDTD simulations to precisely define these detectors which convinced us of the advantage of the RCWA method. Indeed, for some of our structures, it was not possible with FDTD to discern completely the transmitted from the reflected signal, giving rise to not completely correct results (we never observed any discrepancy in zero-transmission regions compared to the RCWA method. The only difference was in the intensity of the transmission).